

Every aspect of advanced retinal imaging laser eyewear: principle, free focus, resolution, laser safety, and medical welfare applications

Mitsuru Sugawara, Makoto Suzuki, Manabu Ishimoto, Kinya Hasegawa,
Nobutaka Teshima, Kenji Yasui and Nori Miyauchi

QD Laser, Inc. Keihin Bldg. 1F, 1-1 Minamiwataridacho, Kawasaki-ku, Kawasaki, Kanagawa,
JAPAN 210-0855

ABSTRACT

Retinal imaging laser eyewear has a miniature laser projector inside the frame which provides the wearer with digital image information through the pupil using the retina as a screen. Its principle is based on the geometric optics of the Maxwellian view combined with a parallel and narrow RGB laser beam. A prototype with the trademark of RETISSA[®] was invented with a miniature laser projector inside the glasses frame using a non-axisymmetric free-surface reflecting mirror. The image resolution was measured based on the visual acuity testing using a retinal projected image of Landolt ring for four subjects with the different naked visual acuity of 0.04, 0.5, 0.9 and 1.2. Also, the theoretical image resolution was studied based on the beam propagation simulation under the eyeball model. The results show how to achieve high resolution and free focus in proper balance by adjusting the laser beam characteristics of the beam diameter and divergence. On the laser safety, RETISSA[®] was found to be in the Class I category, which has the safety factor of over 700 in the RGB radiation intensity under the international standard of IEC60825-1. RETISSA[®] also met the thousand times more strict Class I criteria of FDA/CDRH 21CFR1040.10 with the total RGB radiation intensity of less than 0.37 μW , indicating its laser radiation is not considered to be hazardous as stated in the definition of FDA Class I. The experimental evidence that the radiation of RETISSA[®] is equal to or weaker than displays of conventional digital devices also provide its proof of safety, including its long-term use as one of daily digital devices. The potential of retinal laser imaging is mentioned for use in ophthalmology medicine. The current activity on the medical welfare applications as low vision aids and ophthalmic testing equipment is reviewed including clinical research and trials in Japan and Europe.

Keywords: retinal imaging display, RGB laser, eyewear, free focus, AR, laser safety, low vision aid, medical welfare

1. INTRODUCTION

The process of scanning laser light on the retina was first used by Webb et al. in 1980¹ to develop the scanning laser ophthalmoscope (SLO). In the SLO, the laser beam is scanned two-dimensionally through the pupil of the eye onto some part of the retina, and the reflected beam passing back to the outside is detected allowing an image of the retina to be displayed. This technology has been adopted for fundus imaging and retinal function testing in ophthalmic applications^{2,3}. Webb et al. also noted that when the input laser beam was modulated by a video source, the subject would see an image¹.

Based on this concept of scanning an image directly on the retina of the eye, the virtual retinal display (VRD) was invented at the Human Interface Technology Laboratory (HIT Lab) by Thomas A. Furness III in 1991⁴. A tiny spot is focused onto the retina and is swept over it in a raster pattern. Instead of viewing a screen, the user has the image scanned directly into the eye. Two prototypes, a full-color bench mounted and a monochrome portable unit, were assembled with VGA (640 by 480) resolution image at 60 Hz in the '90s⁵. Using these prototypes, the HIT Lab studied virtual reality (VR) and augmented reality (AR) for visual interaction with environments^{6,7} as well as a visual computer interface which enabled low-vision people to have higher visual acuity and reading speed⁸.

In the first decade of 21st century, two companies have made prototypes of VRD as eyewear. Microvision Inc., founded in 1993 based on the technology spun off from the HIT Lab, built a prototype called Nomad Personal Display System with the targeted applications in workplaces⁹. Brother Inc. demonstrated its eyewear named AiRScouter in Brother World JAPAN 2010¹⁰⁻¹². However, both companies never reached commercial production and ceased development in the end, probably because their prototypes with large optics in front of the wearer’s face did not appeal to any customers in any field.

A compact eyewear called “Retinal Imaging Laser Eyewear” with the trademark of RETISSA[®] was invented with a miniature laser projector inside the frame¹³⁻¹⁶. It provides the wearer with digital image information through the pupil using the retina as a screen. Its remarkable features of free focus, universal design, and natural AR will enable a variety of applications from low-vision aids, ophthalmic testing equipment, workplace support, entertainment to the consumer-oriented smart glass.

This paper describes every aspect of this advanced retinal imaging laser eyewear from its principle, focus-free imaging, experimental and theoretical resolution, laser safety to medical welfare applications.

2. RETINAL IMAGING LASER EYEWEAR, RETISSA[®]

In this section, we describe the retinal imaging laser eyewear RETISSA[®] with a compact new optics by showing the principle and configuration of laser retinal projection, a prototype, and its unique features.

2.1 Basic principle and configuration of laser retinal projection

We start with studying the geometric optics of the Maxwellian view to project an image of the light source on the plane of pupil^{17, 18}. We illustrate that the retinal laser imaging under the Maxwellian view combined with a parallel and narrow RGB laser beam realizes focus-free feature, meaning picture clarity is independent of the wearer’s focusing ability and point of focus. Then, we show a standard optics configuration of retinal laser imaging based on RGB lasers.

Maxwellian View

The Maxwellian view is a method of observation in which a converging lens forms an image of the light source in the plane of the eye’s pupil of the observer, instead of looking at the source directly. Its simplest form compared with normal viewing is illustrated in Figure 1. The observer sees the lens uniformly illuminated with light. This optical arrangement makes it possible to choose the point of incidence within the pupil, to minimize the effect of the optical aberrations of the eye and to increase the quantity of light independent of pupil size. Note that the observer does not see the image of the light source on the retina.

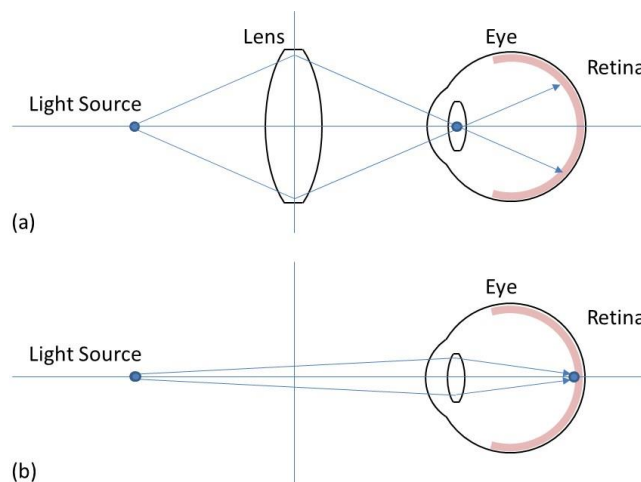


Figure 1. (a) Maxwellian view, and (b) normal viewing

Pinhole Image on the Retina in the Maxwellian View

A method to see the image of the light source in the Maxwellian view is to project the pinhole image at the center of the pupil as seen in Figure 2(a). The thin and parallel light beam through the pinhole from each point of the light source passes through the pupil and reaches the retina. Note that the diffraction at the pin hole is neglected for simplicity. Here, the light beam reaches the retina without using the focusing function of the eye lens, providing a sharp image of the light source. The clarity of the image is independent of the focusing function and the position of the focus of the eye lens, i.e., focus free is realized. The drawback of this is rather a dark image since only a small portion of light comes through the slit from the light source as illustrated in Figure 2(a).

Laser Image on the Retina in the Maxwellian View

Another method to see the image of the light source in the Maxwellian view is to project the laser beam at the center of the pupil as seen in Figure 2(b). The thin and parallel laser beam passes through the pupil and reaches the retina without using the focusing function of the eye lens, providing a sharp image of the light source. The clarity of the image is independent of the focusing function and the focal position of the eye lens, i.e., focus free is realized. Though the principle is quite similar to the pinhole image, the laser image can be much brighter by just tuning the laser power.

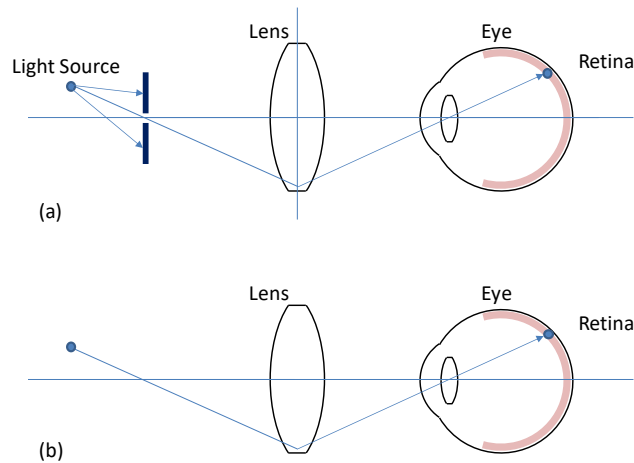


Figure 2. (a)Pinhole and (b) laser beam in the Maxwellian view

Standard Optics Configuration of Retinal Laser Imaging

Based on the discussion above, we know that, by scanning the laser beam synchronized to digital image source around the center of the pupil, a two-dimensional image can be depicted on the retina as the ensemble of the point image. Figure 3 (a) shows a standard configuration of retinal laser imaging. The RGB laser combiner inside the controller provides a laser beam consisting of aligned red, green and blue light, each of which is modulated according to the video signal from the image processor connected to the digital image source. The laser beam is raster-scanned two-dimensionally with the scanning device like a two-axis MEMS mirror being driven by the video signal from the image processor. The spread optical beam converges at the pupil and reaches the retina by the relay optics consisting of two lenses and one reflection mirror, and depicts a two-dimensional image on the retina of the observer as a collection of the point image. The viewing angle can be tuned by the deflection angle of the MEMS mirror. In a word, the retina works as a screen of a laser projector. The clarity of the image is independent of the focusing function and the focal position of the eye lens as long as the laser beam is thin enough (see Section 3), i.e., focus free is realized.

2.2 Prototype

We developed Retinal Imaging Laser Eyewear by replacing the optics of Figure 3(a) consisting of two lenses and one reflector with only one non-axisymmetric free-surface reflecting mirror of Figure 3(b)¹³⁻¹⁶. The free-surface mirror is designed to collimate the RGB semiconductor laser beam scanned by the MEMS mirror and to converge it in the center of the pupil, projecting an image through the pupil onto the human retina.

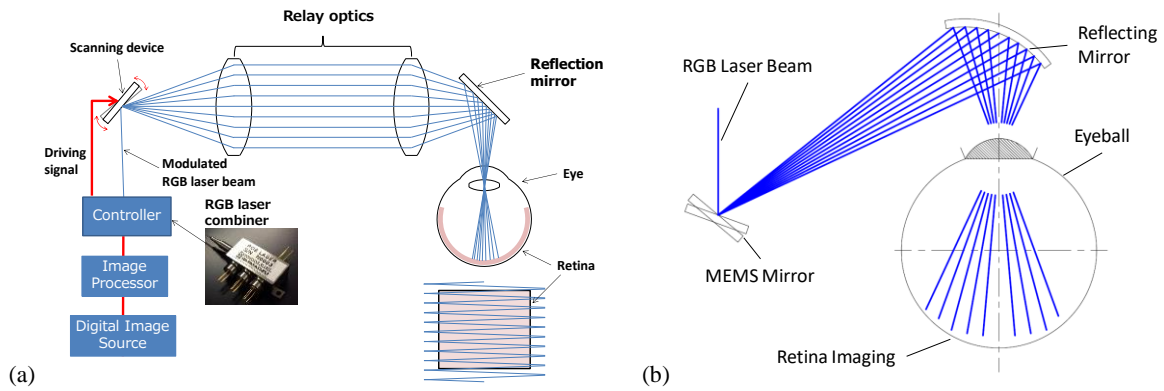


Figure 3. Configuration of retinal laser imaging: (a) standard optics and (b) optics with non-axisymmetric free-surface reflecting mirror



Figure 4. (a) Prototype device with the trademark of RETISSA® (b) RGB digital image by the optics with non-axisymmetric free-surface reflecting mirror

Figure 4 shows the prototype device with the trademark of RETISSA® and the RGB digital image by the optics with non-axisymmetric free-surface reflecting mirror. The RGB laser combiner module inside the controller provides a laser beam consisting of aligned red, green and blue light, each of which is modulated according to the video signal from the image processor connected to the digital image source including the preinstalled camera. The input to the image processor is the HDMI signal of 1280×720×60 Hz (HD 720P). The spread optical beam after the MEMS mirror converges at the pupil and reaches the retina by the free-surface reflecting mirror and depicts a two-dimensional image on the retina of the observer as a collection of the point image. The viewing angle can be tuned up to 40 degrees by increasing the deflection angle of the MEMS mirror.

The ND filter attenuates each laser power to less than 1 μW at the converging point. This laser power assures that RETISSA® belongs to class 1 laser product, which is safe under all conditions of normal use (see Section 4).

The wearer can enjoy laser scanned full-color image from a digital camera installed in the center of the frame as well as from a digital device connected to the controller via the HDMI connector. The weight of eyewear is 57 g.

2.3 Features

The features of RETISSA® is summarized as follows:

1. Focus free, i.e., image clarity is independent of individual focusing function, refractive error, and the focal position of the eye lens,
2. Universal design like normal correcting or sunglasses, owing to small optics inside the glasses frame, and
3. Natural AR, i.e., a digital image is augmented in the real-world environment, independent of the focal position of the wearer since the image is always clear on the retina.

To date, no other wearable devices have achieved these three features whether the devices are using VRDs⁹⁻¹² or conventional liquid color displays¹⁹⁻²¹. These characteristics will enable RETISSA[®] to be used in a variety of application segments from low-vision aids, ophthalmic testing equipment, workplace support, entertainment to the consumer-oriented smart glass.

The resolution of laser retinal imaging is basically determined by the scanned line density and the beam spot size on the retina if we neglect performance limits of the parts like laser response speed, aberration of optics and MEMS scanning frequency etc. Depending on the needs and applications, the optics can be designed to properly balance the resolution and free focus by adjusting the laser beam diameter and divergence as shown in the next section.

3. HIGH RESOLUTION AND FREE FOCUS

This section describes a model, experiments, and simulations on the projected image quality in terms of visual acuity. The results show how to achieve high resolution and free focus in proper balance by adjusting the laser beam characteristics of diameter and divergence

3.1 Model

Eyeball and laser beam

Figure 5 shows the eyeball model for the incident laser beam passing through the pupil to the retina. The incident laser beam is characterized by the beam diameter, d , and the numerical aperture viewed at the cornea defined as

$$NA = \sin\theta_i, \quad (1)$$

where θ_i is the divergence angle of the beam and can be tuned to be positive or negative around $\theta_i = 0$ of the parallel beam.

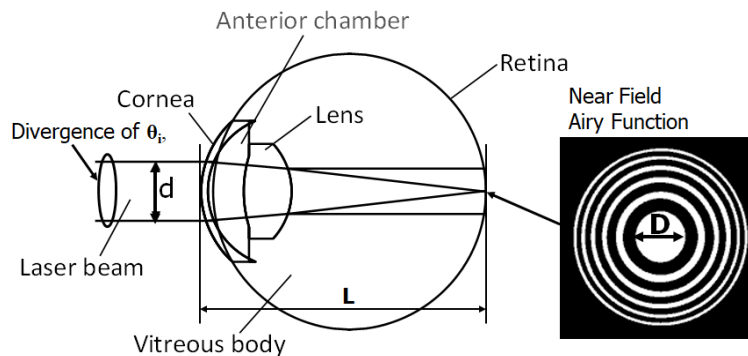


Figure 5. Eyeball model

Based on the beam propagation calculation using the optical simulation software ZEMAX [22], the projected image of the laser beam under the eyeball model was calculated. The eyeball length of L is initially set at 24 mm to provide the focal point on the retina. The value of L can be varied to simulate nearsighted and farsighted eyes. The calculation shows that near-field Airy function appears on the retina with the beam spot diameter, D , as shown in Figure 5.

Figure 6 shows the calculated beam spot radius of $D/2$ as a function of d when $NA = 0$. The blue curve can be approximately given by Rayleigh resolution limit [23] of

$$D/2 = 0.61\lambda / (n \sin\theta_r) \quad (2)$$

where λ is the wavelength of light, n is the index of refraction of the vitreous body, and θ_r is the half angle of the laser beam converging to the retina. For example, the beam diameter of $d = 7$ mm gives $D/2 = 1.5 \mu\text{m}$, and $d = 0.5$ mm gives $D/2 = 21 \mu\text{m}$ for the eyeball with the eye axial length of $L = 24$ mm at the focal point. Note that the diffraction increases D as d decreases.

The orange line of Figure 6 is the beam spot radius of the Gaussian far field pattern calculated under the geometrical optics taking into account the RGB chromatic aberration. The FWHM of the Gaussian is taken as D . We see that the beam spot pattern changes from near-field Airy function to far-field Gaussian around the incident beam diameter of $1.5 \mu\text{m}$.

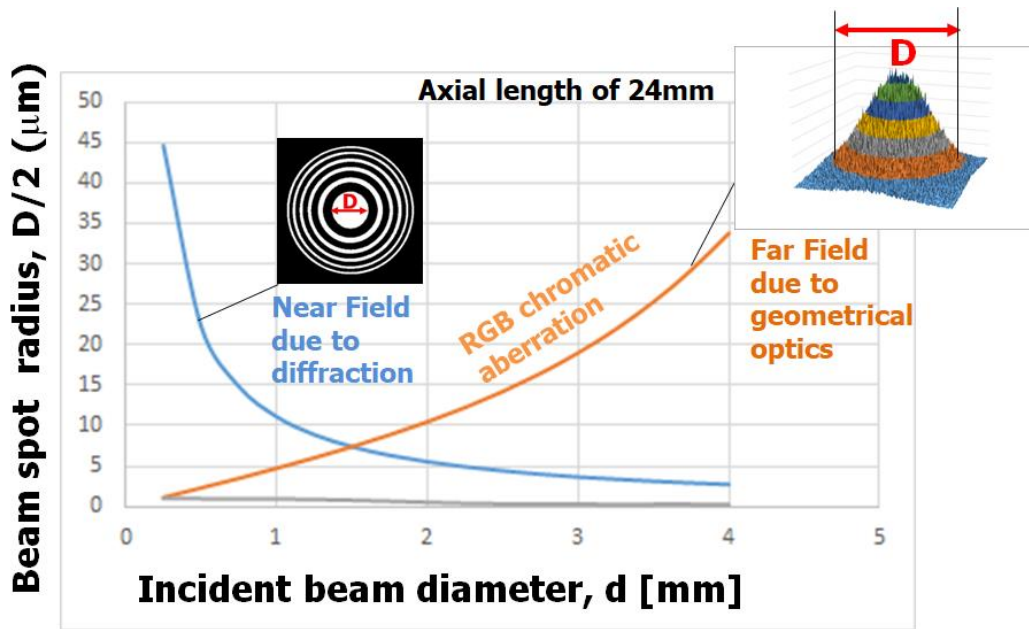


Figure 6 Calculated beam spot radius of $D/2$ as a function of d when $NA = 0$

Acquired visual acuity

It is naturally assumed that the visual acuity acquired by the retinal projection, defined as Acquired VA, is related to D as

$$\text{Acquired VA} = \alpha/D \quad (3)$$

with adjustable parameter, α , to be determined from experiments below.

Scanned line limit

The Acquired VA is limited by the raster scanned line density as

$$\text{Acquired VA} < N/\Phi, \quad (4)$$

where N is the number of vertical scanning lines in the vertical field of view of Φ in the unit of minutes. The point is that, in order to see the Landolt ring at the visual acuity testing, we need to have a line between the separation of the ring.

Depth of Focus

As the incident beam narrows, the depth of focus increases, providing focus-free characteristics of the projected image.

3.2 Experiments

Visual acuity testing using retinal projected image of Landolt ring is done for four subjects with different visual acuity of 0.04, 0.5, 0.9 and 1.2 without correcting glasses, which we call Naked VA. The separation of the Landolt ring spacing on the projected image is calibrated to give the viewing angle of corresponding visual acuity. By changing d and the NA of the incident beam, the acquired VA was obtained for each subject.

Figure 7 shows the picture of the experimental apparatus, which we call “Super Retinal Imaging Display” with variable beam diameter and divergence. The experiment used the setup of $N = 720$ and $\Phi = 11.3 \times 60$ (min) to have, from Eq. (4),

$$\text{Acquired VA} < 1.06. \tag{5}$$

The experimental results of the Acquired VA as a function of the Naked VA for different d and $NA = 0$ are shown in Figure 8 (a), and that for $d = 1.49$ mm and different negative NA in Figure 8 (b). Here, the dots are measured values and lines are guide to the eye.



Figure 7 Experimental apparatus, dubbed “Super Retinal Imaging Display” with variable beam diameter and divergence.

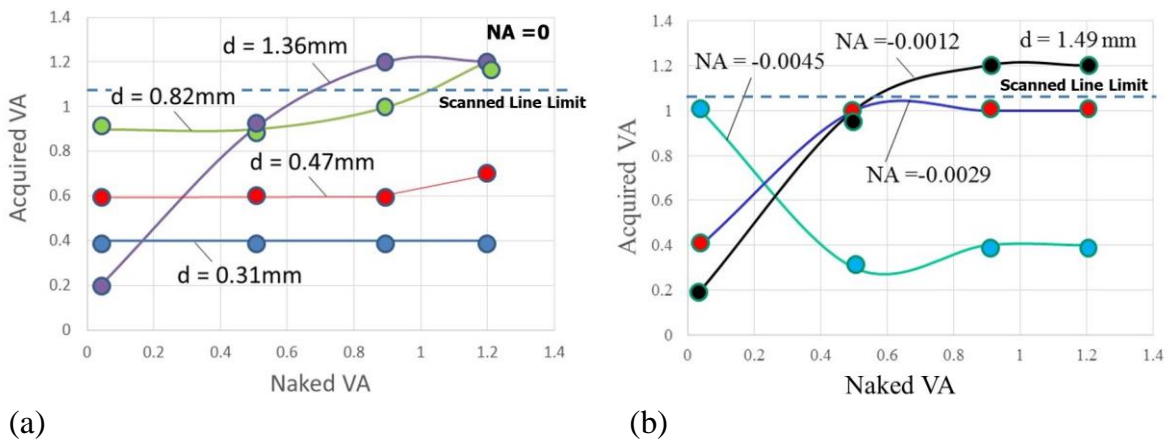


Figure 8 Measured Acquired VA as a function of the Naked VA for (a) different d and $NA = 0$ and (b) $d = 1.49$ mm and different negative NA. The dots are measured values and lines are guide to the eye.

The results tell us

- High visual acuity of above 0.4 with the focus free maintained is realized for the range of $0.31 \text{ mm} < d < 0.8 \text{ mm}$,
- Visual acuity above 0.9 is achieved at $d = 0.82 \text{ mm}$, likely the best balance between resolution and focus free,
- Visual acuity can be tuned for each individual, and
- The maximum visual acuity above 1.0 is possible by adjusting NA to each individual with different Naked VA.

3.3 Simulations

By determining the parameter of α , Acquired VA is simulated as a function of Naked VA as follows.

Parameter, α

Using the Acquired VA of 0.6 at $d=0.47 \text{ mm}$ and $NA=0$ in Figure 8 (a), and the calculated D of 47 mm at $d=0.47 \text{ mm}$ (see Figure 6), Eq. (3) gives

$$\alpha = 28 \text{ } \mu\text{m}. \quad (6)$$

Naked VA

Taking the beam diameter of $d = 3\text{mm}$ corresponding to the pupil diameter under the room light circumstance, the beam spot diameter of D is calculated at an axial length, L . Then the Naked VA at each axial length, L , is given by

$$\text{Naked VA} = \alpha/D(3\text{mm}), \quad (7)$$

where $D(3\text{mm})$ is the beam spot diameter on the retina under $d= 3\text{mm}$ and $NA=0$ at a given eye axial length L . As L increases over 24 mm , $D(3\text{mm})$ increases, and Naked VA decreases, which is the near-sightedness.

Simulations

Using D and $D(3\text{mm})$ at a given L with d and NA as parameters, the relationship between the acquired VA and naked VA can be simulated.

Figure 9 shows the calculated Acquired VA as a function of the Naked VA (solid lines) for (a) different d and $NA = 0$ and (b) $d = 1.49 \text{ mm}$ and different negative NA . The solid dashed lines are guide to the eye for measured Acquired VA in Figure 8. The results show excellent agreement with the measurements in spite of the simple assumption of Acquired and Naked VA.

To summarize, this section clarified the tradeoff relationship between the image resolution and focus free characteristics, i.e. as the beam diameter increases, the beam spot diameter decreases, providing high resolution until the scanned line limit. At the same time, depth of focus decreases, losing focus free. The divergence of the incident laser beam enables providing optimized visual acuity for each individual with different refractive power of the eye lens. We can choose optimum beam characteristics depending what is needed in each application.

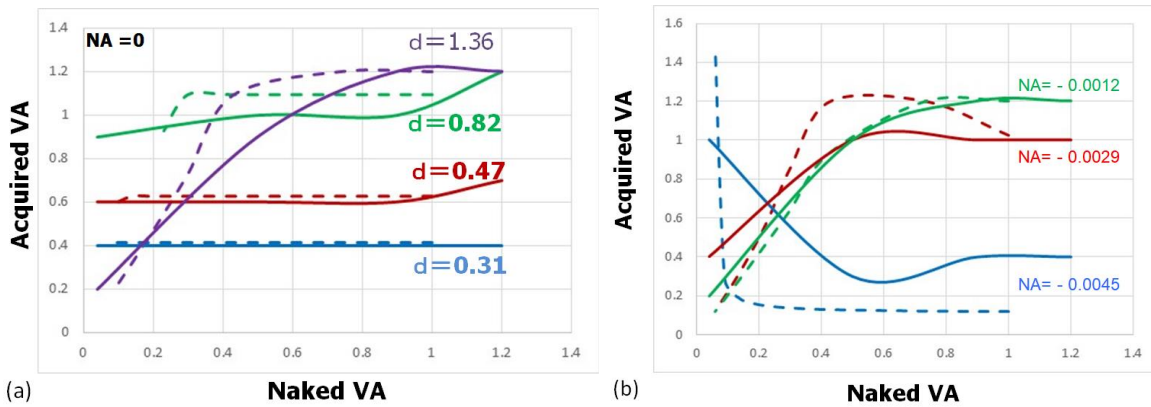


Figure 9 Calculated Acquired VA as a function of the Naked VA (solid lines) for (a) different d and $NA = 0$ and (b) $d = 1.49 \text{ mm}$ and different negative NA . Dashed lines are guide to the eye for measured Acquired VA in Figure 9.

4. CLASS I CLASSIFICATION UNDER IEC/FDA STANDARDS

In this section, we show safety analysis of RETISSA® in terms of the RGB laser radiation intensity based on the international guideline as well as the international and USA standards.

4.1 Exposure limit based on ICNIRP guidelines

The International Commission on Non-Ionizing Radiation Protection (ICNIRP) provides scientific advice and guidance on the health and environmental effects of non-ionizing radiation (NIR) to protect people and the environment from detrimental NIR exposure²⁴. The most recently published guideline for lasers is “ICNIRP Guidelines on limits of exposure to laser radiation of wavelengths between 180nm and 1000µm”²⁵. The purpose of these guidelines is to establish the maximum levels of exposure to laser radiation, called Exposure Limit (EL), which are not expected to cause adverse biological effects to the eyes and the skin. The exposure limits apply to exposure durations between 100 fs and 30 ks (about 8 h) to meet all human exposure to optical radiation emitted by lasers. The ELs were derived on the basis of current knowledge on damage thresholds and in accordance with “ICNIRP Statement: General approach to protection against non-ionizing radiation”²⁶. The guidelines are intended for use by the various experts and national and international bodies who are responsible for developing regulations, recommendations, or codes of practice to protect workers and the general public from the potentially adverse effects of optical radiation. Note that the guidelines say *the biological effects induced by optical radiation are essentially the same for both coherent and incoherent sources for any given wavelength, exposure site, area, and duration*.

According to the guideline, the primary effect on the eye of visible and near infrared radiation (400 to 1,400 nm) is damage to the retina. Because of the transparency of the ocular media and, in particular, the inherent focusing properties of the eye, the retina is much more susceptible to damage by radiation in this spectral region than any other part of the body. In the 400-1,400 nm band, thermal injury to the retina resulting from temperature elevation in the pigmented epithelium is the principal effect for exposure durations less than 10 seconds. Photochemical injury is also the principal type of retinal injury resulting from lengthy exposures (10 seconds or more) to short-wavelength visible radiation (principally “blue light”).

The EL for the photochemical and thermal damage under the exposure time of 30 ks (about 8 hours) is given as follows based on Table 5 of Reference 25 (p. 283). The diameter of the apertures used for averaging exposure levels for the retina is 7 mm, being based on the diameter of a dilated pupil, which provides the most focused light spot on the retina.

Photochemical damage for the wavelength range of 400 to 600 nm is given as

$$EL=39C_B [\mu W], \quad (8)$$

where the correction factors of C_B is given as

$$C_B=10^{0.02(\lambda-450)} \quad (9)$$

from Table 3 of Reference 25 (p.282). Here, λ is the wavelength in nm. Thermal damage in the wavelength range of 400 to 700 nm is given as

$$EL=390 [\mu W]. \quad (10)$$

For the blue laser of 465nm, $C_B=2$, giving the exposure limit due to photochemical damage as

$$EL=77 [\mu W]. \quad (11)$$

For the green laser of 515 nm and the red laser of 640nm, C_B is greater than 10 from Equation (9), giving the exposure limit due to thermal damage as

$$EL=390 [\mu W]. \quad (12)$$

4.2 RGB Laser Radiation Measurement

In the testing of the RGB laser radiation, RETISSA® was operated under the scanning mode with each single color laser emitted continuously. Red, green, and blue digital image was provided as the HDMI input from a computer.

The output of each color was measured by an optical power meter 8230E of ADC Corporation²⁷, with the detector probe set at the converging point for the eye exposure at the cornea.

The measured power in the average, maximum, and minimum power for 17 units is listed in Table I for each color, in comparison with the calculated EL. The standard deviation was 0.005 μW in red, 0.005 μW in green, and 0.003μW in blue. All the measured values were within 10 % of the average. Note that the relative intensity among red, green, and blue lasers have been adjusted to provide optimum white balance when all the lasers are lighted at their maximum.

Table 1 Measured power for each color in comparison with the calculated EL. Measured power shows the average, minimum, and maximum power for 17 units.

Wavelength (nm)	EL (μW) under 8 .3hours	Measured Power (μW)
465	77 Photo chemical	0.060 (0.055 to 0.065)
515	390 Thermal	0.082 (0.075 to 0.091)
640	390 Thermal	0.161 (0.154 to 0.172)

4.3 Class I Classification by IEC 60825-1

The safety of laser products is standardized and outlined by the International Electrotechnical Commission (IEC) document 60825-1²⁸. Here, the laser products are classified based on the calculations of Accessible Emission Limit (AEL) using maximum permissible exposure (MPE). IEC60825-1 is based on the ICNIRP Guidelines²⁵ and MPE is equal to EL in W/cm². AEL is the emission limit of the laser product using MPE for the full open pupil with a diameter of 7 mm, which is equal to EL in W calculated in Section 4.2. The document of EN60825-1 in Europe and JIS C 6802-1 in Japan follows the IEC60825-1.

Table I shows that the measured power of each RGB color is smaller than EL in three orders of magnitude. IEC60825-1 describes how to treat the additive case of more than two wavelengths. In the case of RETISSA[®] using RGB lasers, the safety factor is calculated as

$$\text{Safety Factor} = 1 / (0.06/77 + 0.082/390 + 0.161/390) = 713 \quad (13)$$

Since 713 is above 1, this device belongs to Class 1, which represents lasers that are safe under reasonably foreseeable conditions of operation, including the use of optical instruments for intrabeam viewing as stated in IEC60825-1²⁸.

4.4 Class I Classification by FDA/CDRH 21CFR Part 1040.10

In the United States, compliance with the regulations for lasers and laser products issued by the Center for Devices and Radiological Health (CDRH) of the Food and Drug Administration (FDA) is mandatory. CDRH is responsible for protecting and promoting the public health to assure that patients and providers have timely and continued access to safe, effective, and high-quality medical devices and safe radiation-emitting products²⁹.

The current CDRH regulations pertaining to laser emissions are found in FDA 21 CFR Part 1040 with Sec. 1040.10 Laser products³⁰. The Sec. 1040.10 defines Class I laser product as any laser product that does not permit access during the operation to levels of laser radiation in excess of the AEL, and also, states that Class I levels of laser radiation are not considered to be hazardous. According to the Table I of Reference 30 (see p.668), the Class I-AEL for the emission duration of over 10,000 seconds is 0.39 μW for the wavelength range between 400 and 1400 nm. Note that this Class I-AEL includes 1000 times safety factor to EL of red and green laser thermal damage under the ICNIRP guideline.

The total RGB laser power of RETISSA[®] is given as

$$\text{Total RGB power} = 0.060 + 0.082 + 0.161 = 0.303 \mu\text{W} \quad (14)$$

from Table 1. Since this total power is less than $0.39 \mu\text{W}$, RETISSA[®] is Class I lasers, assuring its laser radiation is “not considered to be hazardous” as stated in the definition of Class I in the FDA/CDRH 21CFR Part 1040.10³⁰

5. COMPARISON OF RADIATION INTENSITY WITH LIGHT IN DAILY LIFE

Comparing the radiation intensity of RETISSA[®] with the light in daily life is expected to provide another proof of safety of this device. This section shows the experimental setup and procedure to realize this comparison in terms of radiation intensity per unit area on the retina, leading to the conclusion that the radiation intensity of RETISSA[®] is equal to or weaker than light in daily life.

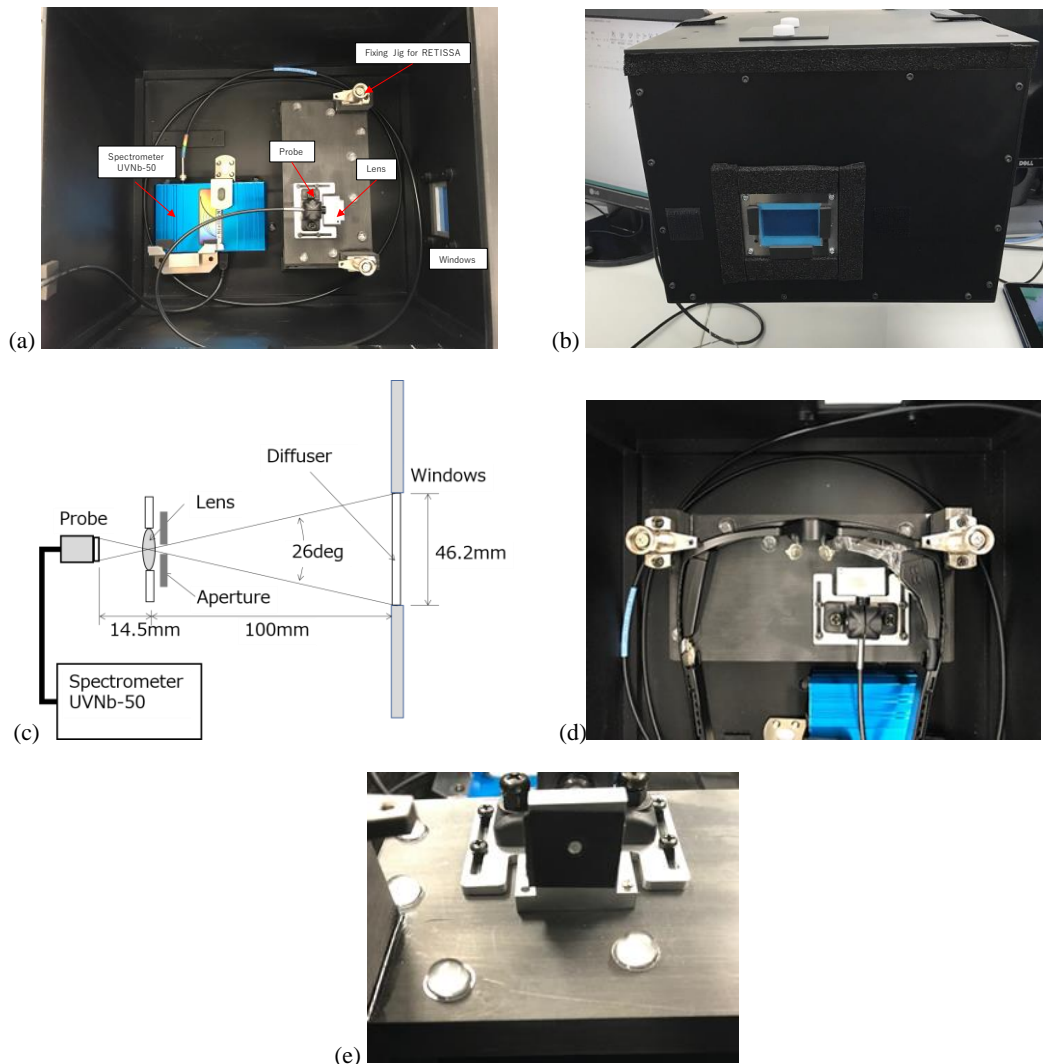


Figure 10 Experimental apparatus to simulate the radiation exposure on retina. (a) photograph of the central part, (b) black box with a windows of diffusion plate, (c) measurement optics, (d) RETISSA[®] set up, and (e) aperture

5.1 Experimental Setup and Procedure

In order to simulate the radiation exposure on retina, we made the experimental apparatus of Figure 11. Figure 11 (a) is the photograph of the central part, which is inside a black box of Figure 11(b) with a windows of diffusion plate. Figure 11(c) illustrates the measurement optics. The light from the outside of the box passes through the diffusion plate of 46.2 mm x 27.1mm, and then, the aperture, and is focused by the lens onto the probe of the spectrophotometer to measure the radiation spectrum of the light. The aperture diameter was chosen to simulate the human pupil (See Appendix C), depending on the brightness of the light. RETISSA[®] can be set in front of the aperture as shown in Figure 11 (d) to coincide its converging point with the center of the lens.

Note that this setup models the human eye with the aperture as the pupil, the convex lens as the crystalline lens, and the detector probe as the retina. The viewing angle from the center of the lens to the diffusion plate is 26 degrees in the horizontal direction and 15.3 degrees in the vertical direction. This viewing angle was chosen to be the same as in RETISSA[®], i.e., the light through the window and from RETISSA[®] provides the same viewing angel of 26 degrees, enabling the comparison of the radiation exposure over the same area of retina.

As the daily light, we used the following items and conditions:

- (a) Sun light at noon under the clear weather,
- (b) Sun light before sunset, with the window toward the sun,
- (c) Sun light at noon under the cloudy weather,
- (d) Fluorescent lamp at the ceiling,
- (e) Tablet
- (f) VR Headset with Smartphone and
- (g) TV LCD display.

The aperture was chosen as 2.0 mm for outdoors of (a) to (c) , 3.0 mm for indoors of (d) and 2.5 mm for the digital devices of (e) to (g) under the white display.

The radiation spectrum was measured by StillerNet UVNb-50 spectrophotometer³¹ between 300 and 800nm with the measurement duration of 5000msec. The radiation intensity was integrated between 400 nm and 700 nm of the visible range.

3.2 Radiation spectrum and intensity

Figure 11 shows the radiation spectrum of RETISSA[®], showing the RGB bright lines of the wavelength of 471, 519.5, and 636.5 nm.

Figure 12 show the radiation spectrum of the above-mentioned daily light in $\mu\text{W}/\text{cm}^2/\text{nm}$, where the spectrum of RETISSA[®] is superimposed. At the right of each spectrum is the integrated intensity as a function of wavelength over 50 nm interval.

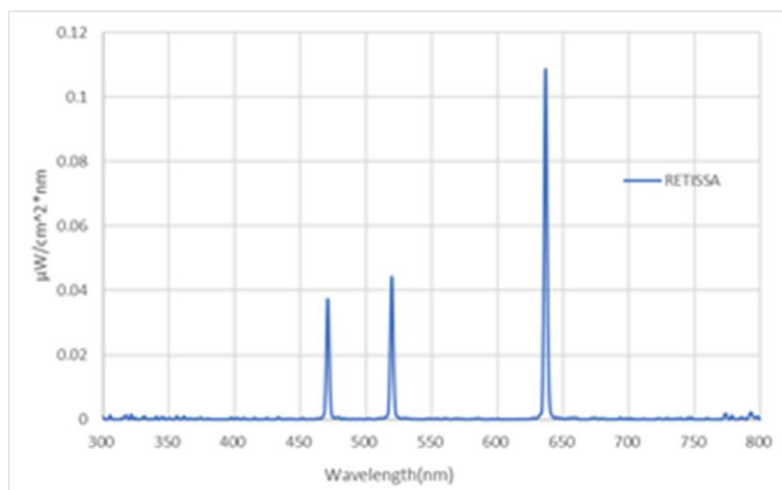
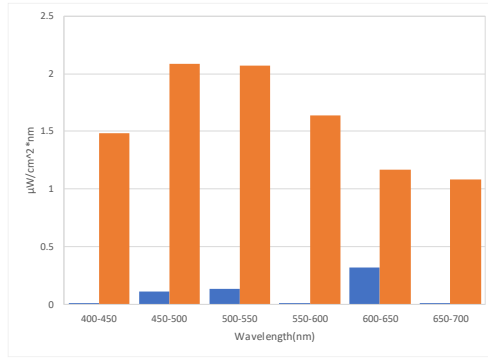
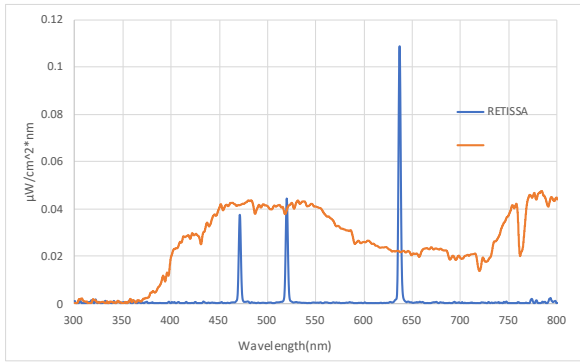
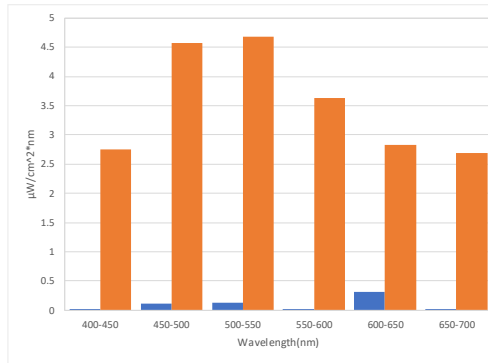
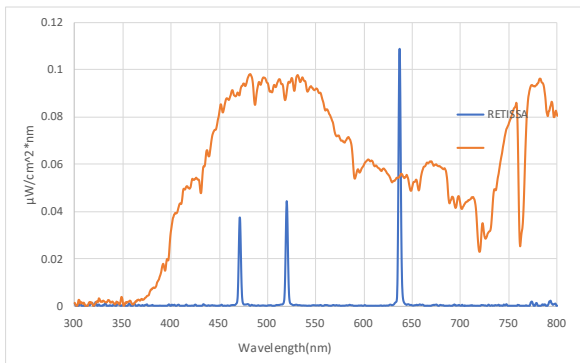


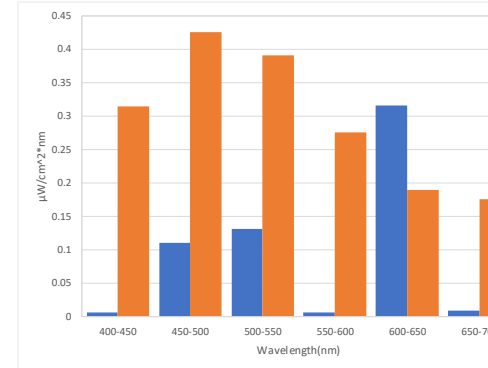
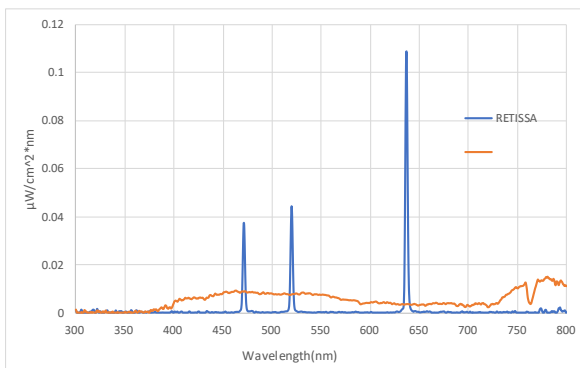
Figure 11 Radiation spectrum of RETISSA[®]



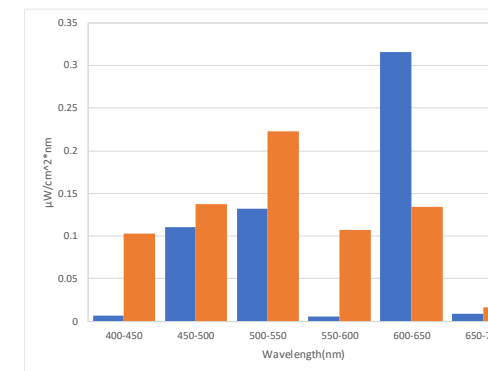
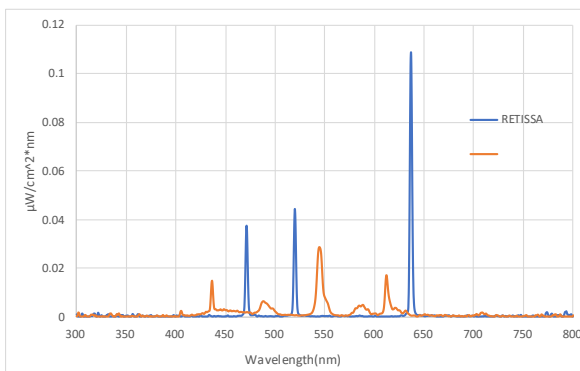
(a) Sun light at noon under the clear weather



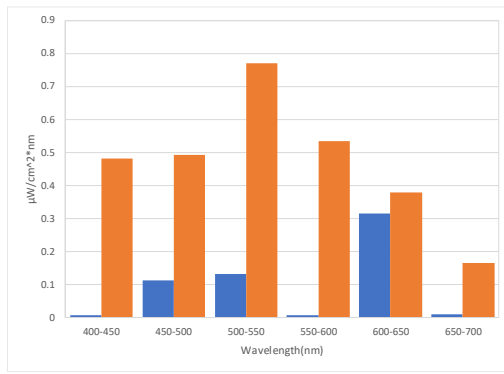
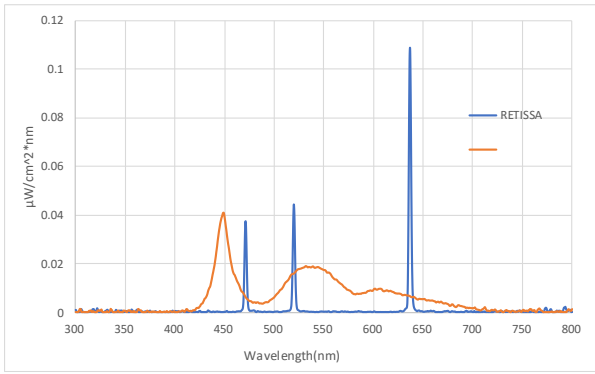
(b) Sun light before sunset, with the plate toward the sun



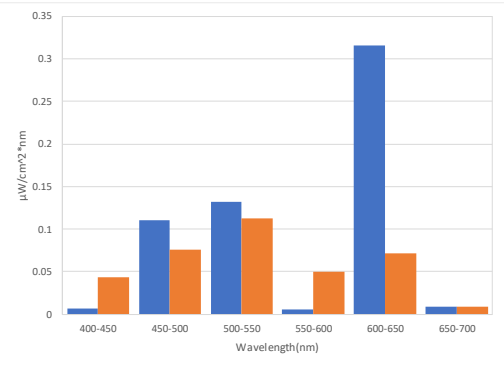
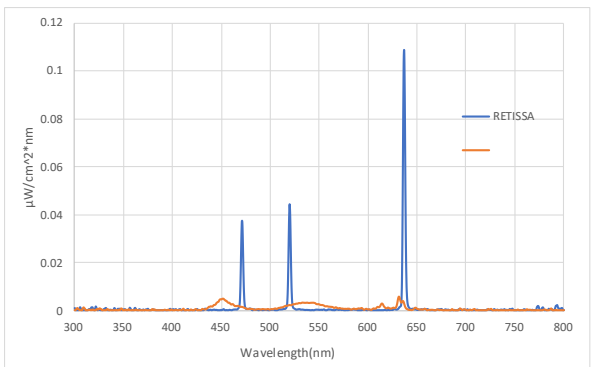
(c) Sun light at noon under the cloudy weather



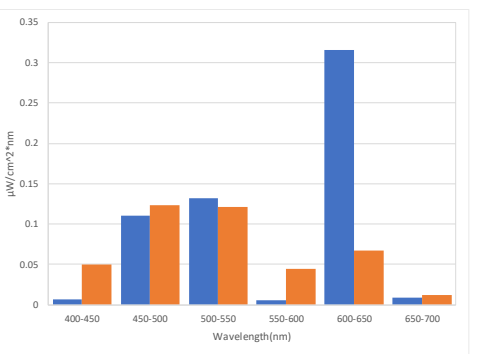
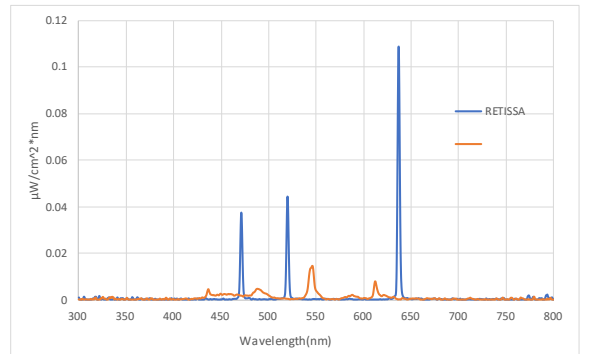
(d) Fluorescent lamp at the ceiling



(e) Tablet



(f) VR Headset with Smartphone



(g) TV LCD display

Figure 12 Radiation spectrum of the daily light in $\mu\text{W}/\text{cm}^2/\text{nm}$, where the spectrum of RETISSA[®] is superimposed. At the right of each spectrum is the integrated intensity as a function of wavelength over 50 nm interval.

Table 2 Integrated intensity of radiation of RETISSA® and the light in daily life over the wavelength range between 400 and 700nm.

Light Source	Radiation Integrated Intensity (μW/cm ²)
(a) Sun light at noon under the clear weather	9.5278
(b) Sun light before sunset, with the plate toward the sun	21.1535
(c) Sun light at noon under the cloudy weather	1.771
(d) Fluorescent lamp at the ceiling	0.722
(e) Tablet under the white display	2.8198
(f) VR Headset with Smartphone	0.3622
(g) TV LCD display	0.4186
RETISSA®	0.5784

Table 2 shows the integrated intensity of radiation of RETISSA® of Figure 11 and the light in daily life of Figure 12. The integrated intensity of radiation of RETISSA® is sufficiently weaker than the sun light under the condition of (a) to (c), and still less than the indoor fluorescent lamp at the ceiling of (d). In particular, note that the sun light intensity of (a) at noon is more than ten times RETISSA, to which the 10%-transmittance sunglasses is not enough to be equal. Although the intensity of the sunlight varies depending on the latitude, the season, the weather and the time zone of the area, we can say that we are receiving light equal to or stronger than RETISSA® on a daily basis. The digital devices of (e), (f) and (g) provide the radiation intensity of the same order as RETISSA, showing that radiation exposure by RETISSA is not much different from widely used digital devices.

RETISSA® with three primary color laser sources has sharp wavelength peaks compared to other light sources. Figure 12 shows that the peak at 636.5 nm corresponding to red has higher strength than green or blue. This red light intensity is needed to achieve the white balance based on the luminosity function of the human eye. As a result, the red peak intensity of RETISSA® is larger than the other light sources of (a) to (f). However, note that the integrated intensity over 50 nm intervals on the right side of Figure 12 is in the same order range.

The thermal damage is dominant in the red wavelength range (see. Section 4.1). Since the retina is constantly cooled by the blood flow and the damage accumulation by the red light saturates at 10 seconds according to Reference 25, there is no reasonable reason to consider long-term damage accumulation by the red week light having a safety factor greater than 2,000 for EL in the international standards (see Table 1).

The radiation emitted from the tablet displaying white (full lighting) at the maximum illuminance is quite strong (Fig. 2 (e)). Also, it has a peak around 450 nm since the light source is a blue LED and a yellow phosphor. Photochemical damage dominates in this wavelength region (see Section 4.1). RETISSA® adopts longer wavelength light source of 465 nm to minimize the influence of blue light and secures the integrated intensity much weaker than the tablet in the blue wavelength region of 450 nm.

This section experimentally evaluated radiation intensity and spectrum of retinal imaging laser eyewear as the RGB laser product, and the light in daily life. The retinal imaging laser eyewear was found to be the Class I laser product which has the safety factor of over 700 in the RGB radiation intensity under the international standard of IEC60825-1. This product also met the thousand times more strict Class I criteria of FDA/CDRH 21CFR1040.10 with the total RGB radiation intensity of less than 0.37 μW, indicating its laser radiation is not considered to be hazardous as stated in the definition of Class I. The light in daily life was measured and compared with the retinal imaging laser eyewear using the newly designed apparatus to model the radiation exposure on the human retina within the same field of view angle of 26 degrees. The radiation of the eyewear was found to be equal to displays of digital devices like a tablet, iphone, and TV LCD, and indoor fluorescent lamp at the ceiling, and a few to twenty times weaker than the outdoor sunlight under

various weather conditions in the visible spectral range of 400 to 800 nm. All these results provide proof of safety of retinal imaging laser eyewear, including its long-term use as one of the daily digital devices.

6. APPLICATION TO OPHTHALMOLOGY MEDICINE AND LOW VISION AID

The retinal laser imaging has potential for use in ophthalmology medicine, since it enables

1. Enhancement of visual acuity for anterior ocular segment disease owing to free focus,
2. Direct access to retina to provide better sight for retinopathy by digitally optimizing or enhancing image,
3. Direct access to retina to diagnose retinal visual function,
4. Handy and wearable devices not only for low vision aids but a variety of ophthalmic testing equipment, and
5. Diagnosis of retinal visual function and disease simultaneously, when hybridized with conventional laser diagnosis like SLO and OCT.

Low vision is defined as the best-corrected visual acuity less than 0.3 in the better-seeing eye. Low-vision people are estimated to be 6,280,000 in Japan, Europe and the United States, and 250 million worldwide according to WHO statistics. Low vision causes difficulty in maintaining their independence and completing typical day-to-day activities since conventional low vision aids like a telescope, magnifying glass, and video magnifiers are hard to improve quality of life.

Focus independent direct projection onto retina makes RETISSA[®] unique as accessibility technology for people with visual impairment especially in the anterior ocular segment. They can access to the real world by the camera capturing an image or digital information via HDMI input, as far as their retina remains working even partly. Natural appearance with universal design in mind makes it truly accessible to all persons without hesitation to use in daily life.

The clinical research and trial of RETISSA[®] as the low vision aid is now being put into practice in Japan and Europe in the year of 2018. A prototype of new ophthalmic testing equipment has already been designed and manufactured. All these results will be presented in the very near future.

7. CONCLUSIONS

Retinal Imaging Laser Eyewear has a miniature laser projector inside the frame which provides the wearer with digital image information through the pupil using the retina as a screen. A prototype with the trademark of RETISSA[®] was invented with a miniature laser projector inside the glasses frame using a non-axisymmetric free-surface reflecting mirror. This paper described every aspect of Retinal Imaging Laser Eyewear from its principle, focus-free imaging, experimental and theoretical resolution, safety, and medical welfare applications.

Its principle is based on the geometric optics of the Maxwellian view combined with a parallel and narrow RGB laser beam. The image resolution was measured based on the visual acuity testing using a retinal projected image of Landolt ring for four subjects with the different naked visual acuity of 0.04, 0.5, 0.9 and 1.2. Also, the theoretical image resolution was studied based on the beam propagation simulation under the eyeball model. The results show how to achieve high resolution and free focus in proper balance by adjusting the laser beam characteristics of the beam diameter and divergence. On the laser safety, RETISSA[®] was found to be in the Class I category, which has the safety factor of over 700 in the RGB radiation intensity under the international standard of IEC60825-1. RETISSA[®] also met the thousand times more strict Class I criteria of FDA/CDRH 21CFR1040.10 with the total RGB radiation intensity of less than 0.37 μ W, indicating its laser radiation is not considered to be hazardous as stated in the definition of FDA Class I. The experimental evidence that the radiation of RETISSA[®] is equal to or weaker than displays of conventional digital devices also provide its proof of safety, including its long-term use as one of the daily digital devices. The potential of retinal laser imaging was mentioned for use in ophthalmology medicine. The current activity on the medical welfare applications as low vision aids and ophthalmic testing equipment was reviewed including clinical research and trials in Japan and Europe.

The features of free focus, universal design like normal correcting or sunglasses, natural AR will enable RETISSA[®] to be used in a variety of application segments from low-vision aids, ophthalmic testing equipment, workplace support, entertainment to the consumer-oriented smart glass.

REFERENCES

- [1] Webb, R. H., Hughes, G. W. and Pomerantzeff, O., "Flying spot TV ophthalmoscope," *Applied Optics* 19(17), 2991-2997 (1980).
- [2] Ellingford, A., "The Rodenstock scanning laser ophthalmoscope in clinical practice," *J. Audiov Media Med.* 17(2), 67-70 (1994).
- [3] Varano, M. and Scassa, C., "Scanning laser ophthalmoscope microperimetry," *Semin. Ophthalmol.* 13(4), 203-209 (1998).
- [4] Furness III, T. A. and Kollin, J.S., "Virtual Retinal Display," US 5467104 A.
- [5] Lin, S-K. V., Seibel, E.J. and Furness III, T.A. "Virtual Retinal Display as a Wearable Low Vision Aid," *International Journal of Human-Computer Interaction*, 15(2), 245-263 (2003).
- [6] Chinthammit, W., Burstein, R., Seibel, E. and Furness, T., "Head tracking using the Virtual Retinal Display," *Second IEEE and ACM International Symposium on Augmented Reality*, October 29-30, 2001, New York, (2001).
- [7] E. Viirre, H. Pryor, S. Nagata, and T. A. Furness III, "The Virtual Retinal Display: A New Technology for Virtual Reality and Augmented Vision in Medicine," *Proc. Medicine Meets Virtual Reality*, San Diego, California, USA, 252-257 (1998).
- [8] Kleweno, C.P., Seibel, E.J., Viirre, E.S., Kelly, J.P. and Furness III, T.A., "The Virtual Retinal Display as an Alternative Low Vision Computer Interface: Pilot Study," *Journal of Rehabilitation Research and Development*, 38(4), 431-442. (2001).
- [9] "Microvision Ships First Nomad Personal Display Systems,"
<http://www.pdacortex.com/microvision_nomad.htm>
- [10] Davies, C., "Brother AiRScouter AR retina scanning display demonstrated," 21, Jul 2010,
<<http://www.slashgear.com/brother-airscouter-ar-retina-scanning-display-demonstrated-2194844/>>
- [11] Watanabe, M., Takayama, H., Asai, N., Matsuda, R., and Yamada, S., "Hyper-Realistic Retinal Scanning Display with Wavefront Curvature Modulator," *Proc. IDW 02*, 1253-1256 (2002).
- [12] Watanabe, M., Takayama, H., Asai, N., Matsuda, R., and Yamada, S., "A retinal scanning display with a wavefront curvature modulator," *J. SID* 11(3), 511-515 (2003).
- [13] Sugawara, M., Suzuki, M. and Miyauchi, N., "Retinal Imaging Laser Eyewear with Focus-Free and Augmented Reality," *Proc. The 23rd International Display Workshops in conjunction with Asia Display 2016*, INP1-2 (2016).
- [14] Suzuki, M., Yasui, K., Hasegawa, K., Miyauchi, N. and Sugawara, M., "Image Quality of Retinal Projection Laser Eyewear: How to Achieve High Resolution and Free Focus in Proper Balance," *Proc. The 6th Laser Display and Lighting Conference (LDC 2017)*, LDC2-3(2017)
- [15] Sugawara, M., Suzuki, M., Ishimoto, M., Hasegawa, K. and Miyauchi, N., "Every Aspect of Advanced Retinal Imaging Laser Eyewear: Principle, Free Focus, Resolution, Safety, and Medical Welfare Applications," *Proc. IDW '17*, 1176-1179 (2017).
- [16] Sugawara, M., Suzuki, M., Miyauchi, N. and Ishimoto, M., "Innovative Display Technology for Low Vision Aid and Medical Application," *Proc. IDW '17*, 1353-1355 (2017)..
- [17] Maxwell, J. C., "On the Theory of Compound Colours, and the Relations of the Colours of the Spectrum," *Phil. Trans. R. Soc. Lond.* 150, 57-84 (1860).
- [18] Westheimer, G., "The Maxwellian View," *Vision Res.* 6, 669-682 (1966).
- [19] Furht, B., [Handbook of Augmented Reality], Springer (2011).
- [20] Schmalstieg, D. and Hollerer T., [Augmented Reality: Principles and Practice], Mark L Taub (2016)
- [21] Peddie P. [Augmented Reality: Where We Will All Live], Springer (2017).
- [22] <<http://www.zemax.com/>>
- [23] For example, < <https://cnx.org/contents/9ANhisjh@5/Limits-of-Resolution-The-Rayleigh>>
- [24] The International Commission on Non-Ionizing Radiation Protection (ICNIRP) <<http://www.icnirp.org/>>
- [25] ICNIRP Guidelines on limits of exposure to laser radiation of wavelengths between 180 nm and 1000 μm , *Health Phys.* 105(3), 271-295 (2013).
- [26] ICNIRP Statement : General approach to protection against non-ionizing radiation. *Health Phys.* 82, 540-548 (2002).
- [27]<<http://www.adcmt-e.com/en/products/opm/8230e/index.html>>

- [28] IEC 60825-1:2014 Safety of laser products - Part 1: Equipment classification and requirements.
- [29]<<https://www.fda.gov/aboutfda/centersoffices/officeofmedicalproductsandtobacco/cdrh/>>
- [30]<<https://www.gpo.gov/fdsys/pkg/CFR-2012-title21-vol8/pdf/CFR-2012-title21-vol8-sec1040-10.pdf>>
- [31] <http://www.stellarnet.us/wp-content/uploads/StellarNet-BLUE-Wave-SPEC.pdf>